JOURNAL OF GEOPHYSICAL RESEARCH: SOLID EARTH, VOL. 118, 277–289, doi:10.1002/jgrb.50067, 2013

Switching between seismic and seismo-acoustic harmonic tremor simulated in the laboratory: Insights into the role of open degassing channels and magma viscosity

John J. Lyons,[1,2] Mie Ichihara,[1] Aika Kurokawa,[1] and Jonathan M. Lees[3]

Received 11 September 2012; revised 18 December 2012; accepted 20 December 2012; published 31 January 2013.

[1] Switching between seismic-only harmonic tremor (SHT) and seismo-acoustic harmonic tremor (SAHT) has been reported at few volcanoes worldwide, but its occurrence may indicate important changes in shallow conduit conditions. Switching was simulated in a laboratory experiment in which harmonic signals were produced with a flow-driven valve and compressed air. The harmonic signals were passed through a tank of shear-thinning viscoelastic fluid, and the resulting signals were recorded. At high fluid stiffness, a stable, open conduit was produced, and the harmonic signals generated within the experimental apparatus were efficiently transmitted into the atmosphere. At lower fluid stiffness, bubbling dominated the activity, stable pathways were not generated in the fluid, and HT was not recorded in the atmosphere. These results are compared to observations of switching at Fuego volcano, Guatemala. We conclude that at intermediate magma viscosities, the development of stable degassing pathways open to the atmosphere will allow HT generated in the conduit to be transmitted into the atmosphere. Further, subtle changes in magma properties and supply rate may control whether SHT or SAHT is recorded, providing information about the state of the shallow conduit and vent at active volcanoes.

Citation: Lyons J. J., M. Ichihara, A. Kurokawa, and J. M. Lees (2013), Switching between seismic and seismo-acoustic harmonic tremor simulated in the laboratory: Insights into the role of open degassing channels and magma viscosity, *J. Geophys. Res. Solid Earth*, *118*, 277–289, doi:10.1002/jgrb.50067.

1. Introduction

[2] Tremor is a widely observed and frequently studied signal from active volcanoes and has been documented at volcanoes of nearly all magmatic compositions and associated with activity ranging from passive degassing to sustained plinian columns [*McNutt*, 1994]. Harmonic tremor (HT) is a subclass of volcanic tremor that shows a fundamental peak in spectral energy with additional spectral peaks, or harmonics, spaced at integer multiples of the fundamental frequency. HT has been most frequently observed in seismic records [e.g., *Benoit and McNutt*, 1997; *Mori et al*., 1989; *Schlindwein et al*., 1995]; however, the increasing deployment of low-frequency microphones with seismometers has revealed that some volcanoes radiate HT both into the ground and the atmosphere, which we refer to as seismo-acoustic HT (SAHT) [e.g., *Garcés et al*., 1998; *Lees et al*., 2004; *Lesage et al*., 2006]. In most cases of SAHT, and often within the same period of activity, HT is observed to switch between only being observed in seismic-only HT (SHT) and being observed in both the seismic and infrasound records. Monotonic infrasonic tremor has been reported both with and without associated seismic tremor [*Fee et al*., 2010; *Goto and Johnson*, 2011; *Ripepe et al*., 2010; *Sakai et al*., 1996; *Yokoo et al*., 2008], but we are unaware of observations of AHT without associated SHT.

[3] Many models have been proposed to explain the interaction of conduit, vent, and fluid dynamics that result in the generation of HT. Most models include some sort of repeating trigger mechanism, typically small earthquakes, explosions or fluid flow, often coupled with a resonator or additional mechanism capable of producing a nonlinear feedback that sustains and stabilizes the oscillations [*Chouet*, 1988; *Julian*, 1994; *Lees et al*., 2004; *Lesage et al*., 2006; *Rust et al*., 2008]. One such model relates HT to a pressure cooker in which a pressure-operated valve sits atop a gas-charged chamber, periodically releasing gas as a function of the gas pressure in the chamber [*Lees and Bolton*, 1998]. *Lesage et al*. [2006] proposed that the volcanic system is capable of generating HT in a manner similar to a flow-driven musical instrument, in which a valve is connected to a chamber capable of sustaining resonance. In this model, the pressure oscillations are initiated by gas flowing through a vent or constriction, similar to air blown over the reed of a clarinet or the opening in a

All Supporting Information may be found in the online version of this article.

[1]Earthquake Research Institute, University of Tokyo, Bunkyo-ku, Tokyo, Japan.
[2]Now at Alaska Volcano Observatory, U.S. Geological Survey, Anchorage, Alaska, USA.
[3]Department of Geological Sciences, University of North Carolina, Chapel Hill, North Carolina, USA.

Corresponding author: John J. Lyons, Alaska Volcano Observatory, U.S. Geological Survey, USA. (jlyons@usgs.gov)

2169-9313/13-0/10.1002/jgrb.50067

recorder [*Fletcher and Rossing*, 1998]. Some HT models suggest that sequences of regularly repeating explosions or earthquakes alone can generate HT [*Fehler*, 1983; *Gordeev*, 1993]. However, *Hagerty et al.* [2000] showed that for Arenal HT that standard deviations of explosion repeat times would have to vary less than 1%. Many volcanoes, like Arenal, show sustained HT for many minutes to hours, suggesting that in these systems, repeating events without a stabilizing feedback mechanism are unlikely.

[4] None of the current HT models address the transition between SHT and SAHT. On the basis of our observations of switching between SHT and SAHT at volcanoes Fuego (this work) and Shinmoe-dake [*Ichihara et al*., Switching from SHT to SAHT at a transition of eruptive activity, *submitted to Earth, Planets and Space*, 2012], we developed a laboratory experiment to investigate how volcanoes sometimes produce HT that is only transmitted in the ground, while at other times transmit HT into the ground and atmosphere. Most models of HT rely on theoretical numeric formulations, based on conduit and vent characteristics typically derived from geophysical data. As with all studies of HT, a major limiting factor in constraining and refining the models is lack of direct observations. Although analogue experiments of volcanic processes also have limitations, they are capable of incorporating the physics of numerical models with the generation of actual observations that can be compared to data from volcanoes. The purpose of this paper is not to present another model for how HT is generated within volcanoes, but to focus on explaining what causes the switching between SHT and SAHT, which also has implications for the generation of HT.

[5] Here we present results from a series of experiments in which a harmonic signal is generated by the flow of compressed air through a valve and then passed through a tank of viscoelastic fluid open to the atmosphere. Pressure oscillations are recorded within the tubing and valve system containing only gas, and in the atmosphere above the tank of viscoelastic fluid. We vary the concentration of the fluid and observe a change from bubbling to an open conduit or persistent degassing pathway associated with an increase in fluid stiffness. Analysis of the pressure oscillations generated during bubbling and open conduit regimes shows that signals analogous to SAHT are only generated when a persistent degassing pathway is generated in the viscoelastic fluid. Finally, we compare the experimental results with the seismic and infrasound data in order to relate how changing viscosity and the development of open degassing pathways may affect SHT – SAHT switching in volcanoes.

2. Experimental Background and Setup

[6] The analogue model we used in our experiments contains three main elements: gas flow, a valve-resonator system, and a tank of viscoelastic fluid (Figure 1). Because SAHT is typically observed in association with continuous degassing and minor explosions, we consider the oscillations responsible for HT to be driven by a gas phase that is separated from the magma in the shallow conduit. This experimental constraint requires a specific mechanism in order to excite harmonic oscillations by gas flow. Pressure-control valves allow for sound production in certain musical instruments and animal vocalization [*Fletcher*, 1993] and has also been applied to HT generation in volcanoes [*Lees and Bolton*, 1998; *Lesage et al*., 2006; *Rust et al*., 2008]. Three simple pressure-control valve configurations exist that are all capable of producing sustained oscillations (Figure 2). Fluid flow through a deformable crack corresponds to the (+,+) valve [*Julian*, 1994; *Rust et al*., 2008]. A volcanic vent at or very near the surface [*Lesage et al*., 2006] or the pressure-cooker model of sustained oscillations [*Lees and Bolton*, 1998] represent the (+,-) valve configuration. The valve in our experiment (Figure 2a) is the (-,+) type, analogous to a clarinet reed which is often related to volcanic activity and harmonic oscillations [e.g., *Julian*, 1994; *Lesage et al*., 2006; *Rust et al*., 2008]. In our experiment, the valve is made

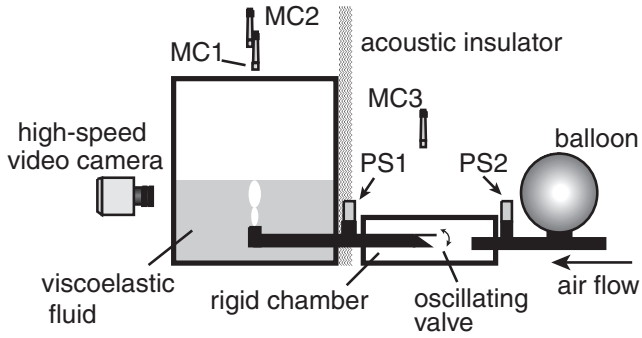

Figure 1. Schematic of the experimental apparatus showing the direction of air flow, the locations of the oscillating valve, in-line pressure sensors (PS1 and PS2), and microphones (MC1, MC2, and MC3). The Plexiglass tank is 230 mm deep with a 200 mm square base. Compressed air passes through the conduit and is injected vertically into the viscoelastic fluid 30 mm from the bottom of the tank. The fluid surface is 40–43 mm above the injection nozzle for the majority of the experimental runs, but the fluid depth was doubled for the deeper fluid experiments.

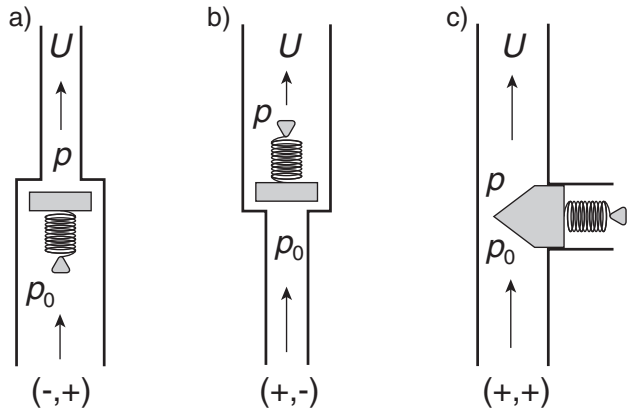

Figure 2. Illustrations of the three types of flow-controlled valves. Arrows indicate direction of flow, U is fluid volume flux, p_o is pressure on the upstream side of the valve, and p is the pressure on the downstream side of the valve. (a) The (−,+) valve opens when the upstream pressure is lower ($p_o<p$). (b) The (+,−) valve opens in the opposite condition ($p_o>p$). (c) The (+,+) valve opens when pressure increases on either side. The figure is modified after [*Fletcher and Rossing*, 1998].

of a thin plastic membrane attached to a 6 mm diameter and 85 mm long tube cut at ~45˚ (Figure 1; Online Supplementary Video 1). This valve design was chosen because it is easy to construct in the laboratory, and we knew from earlier experiments that this valve was capable of producing clear harmonics.

[7] Harmonic oscillations of a pressure-control valve can be produced by steady flow without the aid of a resonator [*Julian*, 1994; *Rust et al*., 2008]. However, in many musical instruments and models of volcanoes, a resonator is combined with the valve to stabilize the oscillations [*Fletcher and Rossing*, 1998; *Lesage et al*., 2006]. In the case of the (-,+) valve, the resonator works to stabilize the oscillations only when its resonant frequency is lower than the natural frequency of the valve [*Fletcher and Rossing*, 1998]. We added an elastic chamber to the rigid conduit of our experiment (Figure 1) to lower the resonance frequency of the system below the natural frequency of the valve. In the actual volcanic conduit at magmatic temperature and pressure, the conduit and magma provide this elasticity. In experiments performed without the balloon, the system generated no sustained oscillations.

[8] Distinct from previous models that assume the valve is located at the surface [*Lees and Bolton*, 1998; *Lesage et al*., 2006], the valve in our experiment is located beneath a chamber of viscoelastic fluid (Figure 1). The experimental design was inspired by *Divoux et al*. [2009, 2011], who showed that gas flow rate and non-Newtonian fluid rheology are the main controlling factors for gas transport mechanism (bubbling or open conduit). They also showed that in a limited intermediate range of gas flow rates and the fluid stiffnesses, the system spontaneously changes between bubbling and open conduit regimes without changes in either gas flow or fluid concentration. Furthermore, *Divoux et al*. [2011] showed accumulation of trapped bubbles plays an important role in the internal evolution of effective rheological property to cause the transition from bubbling to open conduit at a fixed flow rate. We hypothesize that a similar transition in the shallow conduit of active volcanoes may be responsible for the observed transitions between SHT and SAHT, although we have yet to understand which rheological properties (viscosity, elasticity, yield strength, etc.) control the transition.

[9] The viscoelastic fluid used in our experiments is a commercially available hair gel ("Gatsby SH Styling Gel", Mandom Corp.) diluted with distilled water. This fluid was chosen because the mixtures are easily reproducible and maintain a stable stiffness in time [*Vidal et al*., 2009]. The non-Newtonian fluid characteristics are easily modified by changing the percentage of water used to dilute the gel, and the shear-thinning rheological property of the fluid is similar to that reported by *Divoux et al*. [2009] (Figure 3). Changing the gel concentration may change other rheological properties such as yield strength and rigidity as well as viscosity. The rheological properties of the gel solution have not been fully characterized, though some information was provided by using the same fluid as *Vidal et al*. [2009]. Throughout this paper, the rheological properties of the gel solution with high and low gel concentrations are represented by high and low stiffness, respectively. Experiments were run with six different fluid stiffnesses, and we report results from the highest and lowest stiffness experiments because they demonstrate the entire range of observed behaviors.

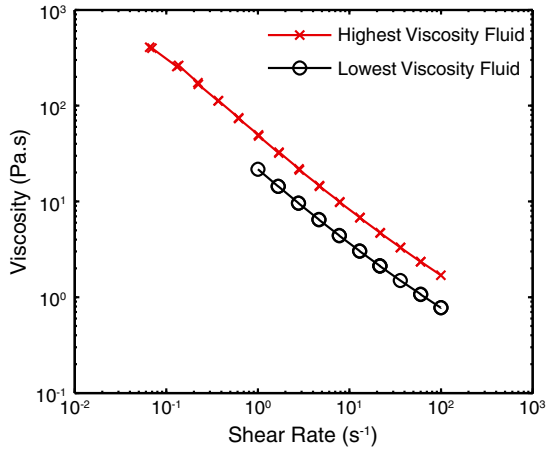

Figure 3. Non-Newtonian viscosity as a function of the shear rate for the highest and lowest stiffness gels used in the experiments. The measurement is performed using a rheometer equipped with cone-plane geometry (40 mm diameter, 4˚cone angle).

[10] The viscoelastic fluid is placed in a 230 mm deep Plexiglass tank with a 200 mm square base. Compressed air passes through the pressure-control valve and is injected vertically into the viscoelastic fluid 30 mm from the bottom of the tank (Figure 1). The surface of the fluid is 40–43 mm above the air injection nozzle for the majority of the experimental runs, but for several runs, the fluid depth was doubled to investigate the effect of a deeper fluid level. Experimental runs typically lasted 1–2 min, with air pressure slowly increased until the valve membrane began oscillating. After sustained oscillation for tens of seconds, the air pressure was varied to observe the results of gas flow with and without oscillation for different fluid viscosities.

[11] Data from experimental runs were recorded by pressure sensors, microphones, a high-speed camera, and a video camera. Two quartz pressure sensors (Kistler 701A with 5011A charge amplifiers) were located within the compressed air conduit, one upstream of the membrane valve (PS2) and one downstream of the valve (PS1). Three condenser microphones (Bruel & Kjaer 4193 + 2669 L with a Nexus 2690 signal conditioner) were placed around the experimental apparatus, two above the center of the tank of viscoelastic fluid (290 mm and 301 mm above the fluid surface) and one located above the chamber housing the flapping valve. The microphone closest to the fluid surface (MC1) recorded signals emitted into the atmosphere most clearly, so we only report data from this microphone. In this experimental and sensor configuration, the signals from PC1 and PC2 are regarded as comparable to seismic signals and the signals from MC1 are comparable to infrasound signals.

[12] Data from the inline pressure sensors and microphones were sampled at 50 kHz by a PC-based data acquisition system (DEWETRON, DEWE-211). A Photron high-speed camera (FASTCAM-1024PCI) was focused on the tank of viscoelastic fluid to capture the nozzle injecting air into the fluid, the rise of the gas through the fluid, and the surface activity resulting from the gas flow (Figure 1). High-speed images were recorded at 10,000 frames per second (fps). In addition, images of experimental runs were recorded with a

digital video camera (SONY Handycam, DCR-TRV900) and saved to a PC at 25 fps. The data acquisition PC, the high-speed camera, and the video-capturing PC were all synchronized.

3. Experimental Observations

[13] In the following, we present results from our experimental runs. Three scenarios are reported because they represent all the experimental variation observed: (1) the highest stiffness fluid at a normal fluid level, (2) the lowest stiffness fluid at the normal fluid level, and (3) the lowest stiffness fluid at the deeper fluid level.

3.1. High Stiffness Fluid

[14] Experiments run with the highest stiffness fluid only produce significant signals in the pressure sensors and microphones when the valve is oscillating. Three distinct types of activity are observed during air flow with valve oscillation: (1) bubbling, (2) an open conduit in the fluid connecting the air nozzle and the atmosphere, and (3) transition between bubbling and an open conduit (Online Supplementary Video 2). Figure 4 shows waveforms for each type of activity observed in the high stiffness fluid with valve oscillation in sensors PS1, PS2, and MC1 as well as a frame from the high-speed camera showing features of each phase of activity in the viscoelastic fluid. Pressure oscillations at PS1 are characterized by high amplitude rarefactions corresponding to valve closure. High amplitude compressions in PS2 are in phase with PS1 rarefactions and also occur regularly as the oscillating valve closes.

[15] During the bubbling phase (Figures 4a and 4b), high amplitude pulses are recorded in MC1 when a bubble grows to reach the surface. The pressure signal recorded in MC1 is thus due to temporary connectivity between the air nozzle and the atmosphere, not to bubble bursting. The bubbles grow in a pulsatory manner corresponding to valve oscillation, and several small pressure transients in MC1 often precede bubble bursting. These appear to be due to the oscillation of a small residual bubble interacting with the pulsatory growth of the next bubble as it nears the fluid surface (Figure 4b). When bubbles are growing, the pressure pulses in PS2 show an initial compression associated with valve closure, followed by subsequent peaks of the same frequency but lower amplitude (Figure 4a). The oscillations following valve closure are governed by the resonance of the entire system (the balloon, tubing, rigid container, and the bubble or conduit in the fluid).

[16] After a period of bubbling and an unsteady transition between bubbling and an open conduit (Figures 4c and 4d), a stable, open conduit forms (Figure 4f), and valve oscillations are transmitted uninterrupted into the atmosphere (Figure 4e). To investigate the differences between the bubbling and open conduit regime, a 10 s continuous record that spans the three regimes presented in Figure 4 is evaluated by calculating the time between successive pulses (ΔT Pulse) and the maximum cross-correlation coefficient (MaxXcorr) between successive pulses at PS1 (Figure 5). The bubbling regime shows the highest variability in duration between valve oscillation and resulting waveforms. The time between pulses begins to stabilize, and waveform similarity increases as bubbling transitions toward an open conduit. Once the open conduit is established (at ~8 s, Figure 5), the time between pulses becomes very regular, and the waveforms are effectively identical.

[17] Spectrograms of MC1, PS1, and PS2 were calculated for the same 10 s period as in Figure 5 and reveal additional information about how the different regimes affect the regularity of the valve oscillation and transmission of the signal into the atmosphere (Figure 6). All spectrograms of the experimental data were calculated with a fast Fourier transform on data downsampled to 5000 samples per second using a window length of 512 samples with a 256 sample overlap. The continuous oscillation of the valve during bubbling, transitional, and open conduit regimes is clear in the conduit pressure sensors PS1 and PS2. The fundamental frequency is strong during bubbling, but the irregularity in valve oscillation results in a broad swath of spectral energy instead of clear harmonics (Figures 6b and 6c). The fundamental oscillation of the valve is also captured in the atmosphere (Figure 6a), but the intermittent connection with the compressed air nozzle during bubble bursts is clear in the vertical stripes in the first several seconds of spectra from MC1. In all three sensors, the harmonics become better defined as bubbling moves into the transition regime, but clear, well-defined harmonics are only observed when a stable, open conduit has formed.

3.2. Low Stiffness Fluid

[18] Unlike with the high stiffness fluid, pressure transients are generated during air flow with and without valve oscillation in the low stiffness experiments. The low stiffness fluid prevents the formation of a sustained open conduit in the fluid, and activity is dominated by the formation of bubbles (Online Supplementary Video 3). High amplitude signals are produced in the atmosphere in the low stiffness experiments by bubble oscillation at the surface. There are two types of bubble oscillation: (1) free oscillation excited by detachment from the conduit nozzle and (2) bubble head oscillation while still attached to the conduit nozzle (Figures 7c and 7d).

[19] During the bubbling regime without valve oscillation, bubbles detaching from the conduit nozzle are the only source of high amplitude signals in the conduit pressure sensors and the microphones (Figures 7a and 7b). In these experiments, bubbles extend to the surface and begin to expand while still attached to the conduit nozzle. High-speed video shows that high amplitude pressure transients occur in all three sensors at each occurrence of bubble detachment from the conduit nozzle (Figures 7a and 7b). Both PS1 and PS2 show positive pressure pulses following bubble separation from the nozzle, attributed to the sudden pressure increase, while MC1 shows an initial rarefaction, both of which we attribute to surface tension. The effective conduit volume decreases due to rapid shrinkage of the stretched air–fluid interface into the conduit, while the fluid surface suddenly drops (movement away from MC1) as a reaction to the rapid upward motion of the extended tail of the bubble. Subsequent expansion and oscillation of the bubble at the fluid surface prior to bursting is responsible for the ~0.04 s pressure oscillation in MC1 that is absent in the conduit pressure sensors (Figure 7a). As in the case of high stiffness bubbling, the bursting of the bubble produces no pressure signal above the background noise.

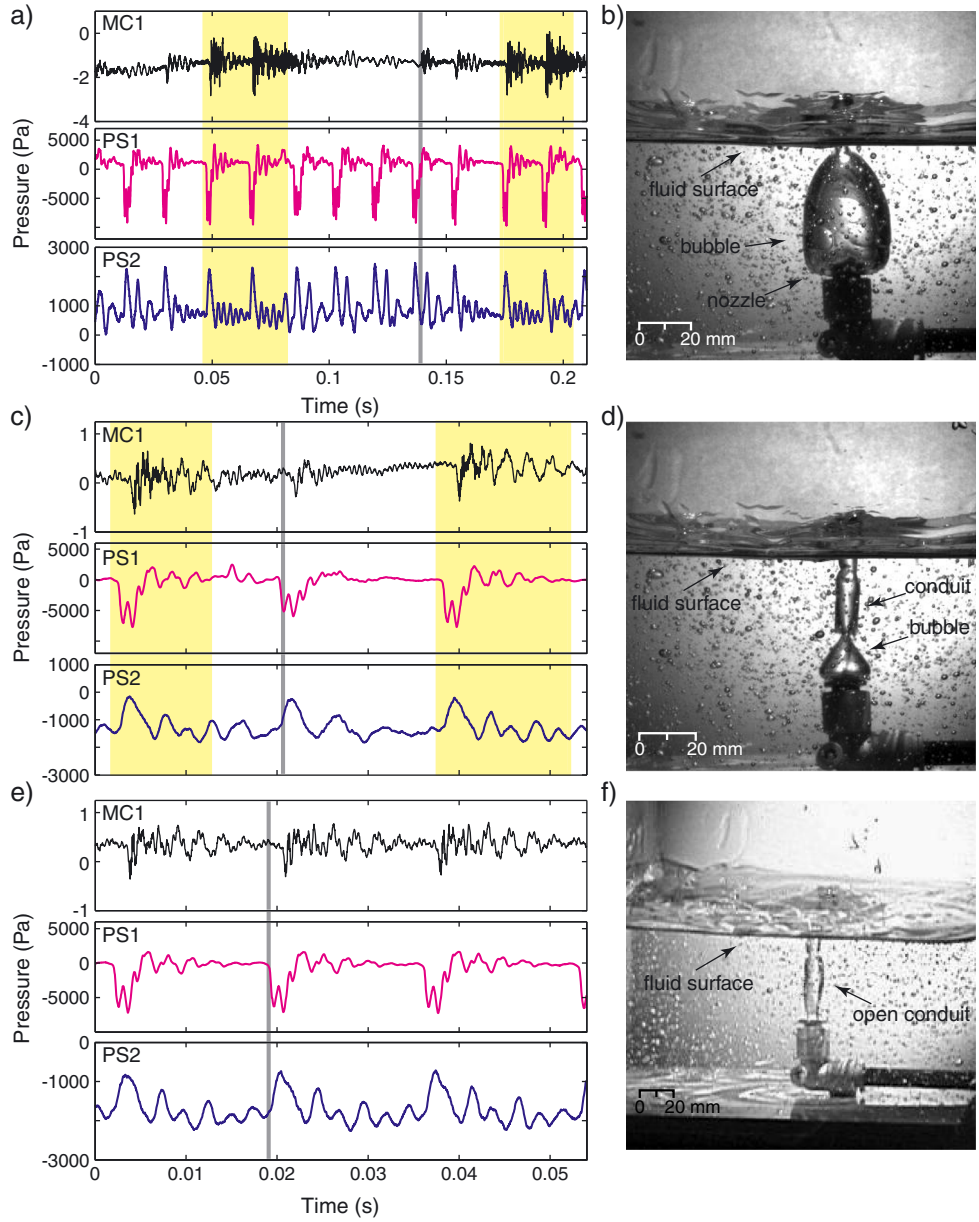

Figure 4. Waveforms and images of the three types of activity observed for experimental runs with the highest stiffness fluid and constant valve oscillation: (a,b) bubbling regime, (c,d) transition from bubbling to open conduit regime, and (e,f) stable, open conduit regime. Waveforms are shown for the microphone closest to the fluid surface (MC1) and both in-line pressure sensors (PS1 and PS2). Gray vertical line through waveforms indicates timing of image associated with that activity at right. Regular pressure transients are observed during all types of activity in PS1 and PS2 due to valve oscillation. The yellow boxes in Figures 4a and 4c indicate when temporary connections between the nozzle and the atmosphere are formed. Irregular pressure signals are observed in MC1 only in these periods. Once a stable, open conduit has formed in the fluid in Figure 4f, every valve oscillation produces a regular pressure pulse in the atmosphere in Figure 4e.

[20] The onset of valve oscillation with bubbling produces pressure pulses in the conduit similar to those recorded in the experiments with high stiffness fluid (Figure 7c). The main effect of valve oscillation on the bubbling signal recorded at MC1 occurs when the bubble breaches the fluid surface while still remaining attached to the conduit nozzle (Figure 7d). Actuation of the valve in this bubble configuration results in a high amplitude, low-frequency oscillation of the bubble head (Figure 7c). The frequency of this initial bubble oscillation is lower than that after bubble detachment because the effective bubble size is much larger while it is still connected to the conduit nozzle. Following the valve oscillation signal, the bubble detaches and generates a signal in all three sensors that is very similar to the bubble detachment signal produced without valve oscillation (Figures 7a and 7c). The bubble detachment

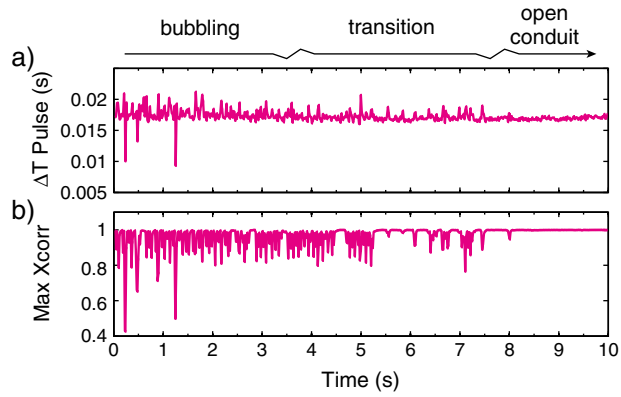

Figure 5. (a) Time interval (ΔT) and (b) maximum cross-correlation coefficient (MaxXcorr) between successive valve oscillation pulses recorded at PS1 during a 10 s record spanning the three types of activity generated in the high stiffness experiment (Figure 4). Bubbling shows the highest variability in timing and waveforms but transitions to nearly identical, evenly spaced waveforms as an open conduit develops.

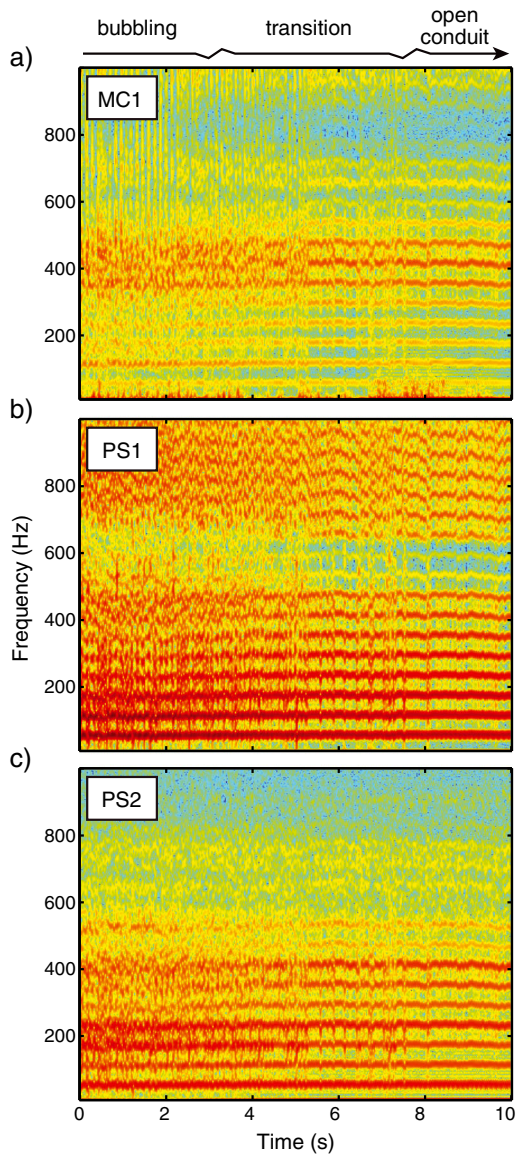

Figure 6. Spectrograms of data from (a) MC1, (b) PS1, and (c) PS2 during the same period of activity shown in Figure 5. During bubbling, the fundamental frequency of valve oscillation is clearly recorded in the in-line pressure sensors in Figures 6b and c, but the intermittent connections with the atmosphere produce the vertical stripes seen in Figure 6a and prevent the generation of clear harmonics in all Figures 6a to 6c. The clear harmonics are only seen when the stable, open conduit is formed.

signal can be seen clearly in PS1 as a positive pulse between rarefactions (Figure 7c).

[21] To compare bubbling and bubbling plus valve oscillation, and how bubble detachment affects valve oscillation, the ΔT between successive bubble releases and valve oscillation pulses was calculated for 10 s of consecutive data at PS1 that covers the activity in Figure 7 (Figure 8a). The MaxXcorr for successive bubble detachment signals and valve oscillation signals was also determined for the same time period (Figure 8b). During the first 5 s of just bubbling, the time between bubble detachments is steady and then slowly begins to decrease as air pressure is increased to initiate valve oscillation (Figure 8a). Despite the changing ΔT, the waveforms generated by bubble detachment are nearly identical during the bubbling regime (Figure 8b). The onset of valve oscillation causes the time between bubble detachments to increase overall and become much more variable. Valve oscillation has a strong effect on the consistency of bubble detachment waveforms (Figure 8b). Individual valve oscillations are not shown as points in Figure 8 for clarity, but on average, eight oscillations occur between every bubble detachment. When a bubble detachment occurs, the effect on the valve oscillation is a sharp drop in waveform correlation and an increase in the time between successive pulses (Figure 8). The temporal disruption in valve oscillation caused by bubble detachment can also be seen in the PS1 trace of Figure 7c.

[22] Spectrograms of MC1, PS1, and PS2 are calculated for the same 10 s period shown in Figure 8 and show the distinct difference in signals from bubble detachments and valve oscillations (Figure 9). Prior to valve oscillation, bubble detachment and oscillation at the fluid surface produces regular but weak signals in the atmosphere. Once oscillation begins, strong signals are recorded in the conduit pressure sensors, but the harmonics are disrupted by bubble detachments. Valve oscillation produces stronger signals in the atmosphere as temporary connections are made from the conduit nozzle to the fluid surface with bubbles (Figure 9a). The temporary connections transmit energy into the atmosphere at integer overtones of the fundamental frequency of the valve oscillation, but do not produce the clear, sustained harmonics seen in the open conduit regime of the high fluid stiffness experiments (Figure 6a). Additionally, pulsatory bubble growth during valve oscillation prior to connection with the atmosphere transmits some energy through the fluid to the atmosphere. This energy is expressed as weak low frequency peaks below 200 Hz in MC1 (Figure 9a). These bubble detachment and oscillation signals are enriched in low-frequency energy, as shown in Figure 9c.

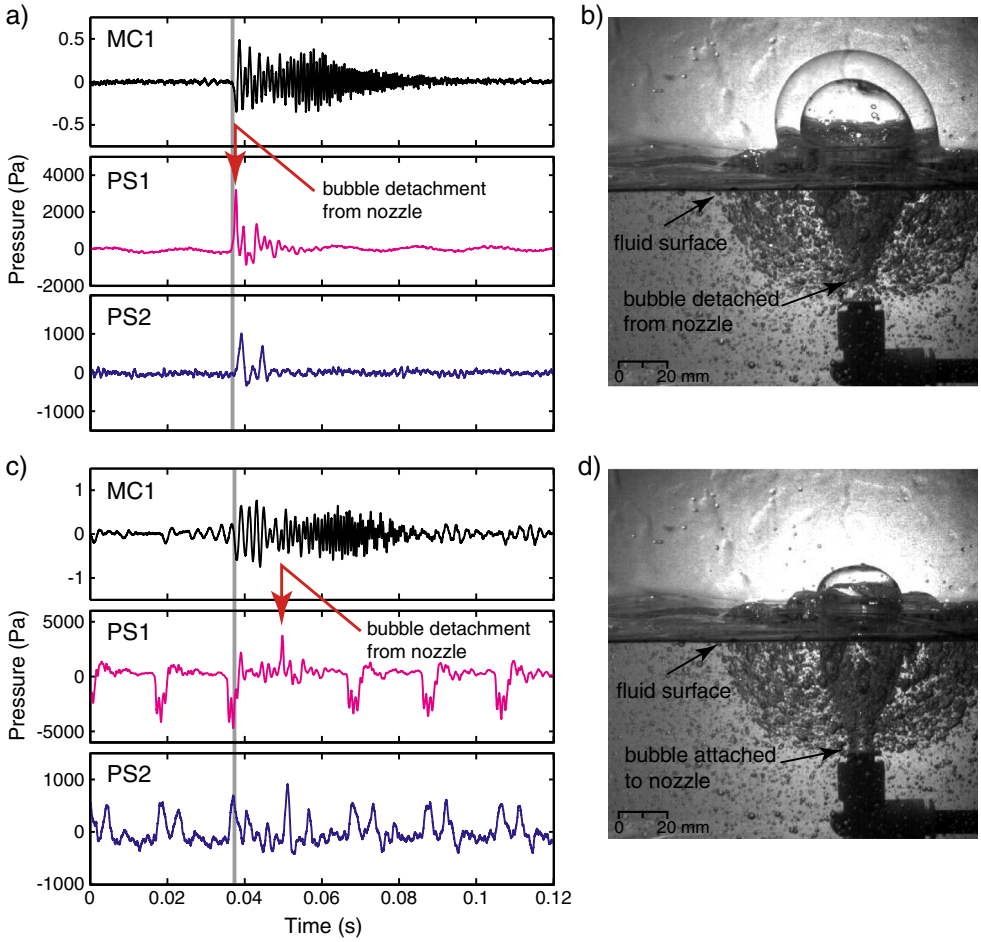

Figure 7. Waveforms and images of bubbling in the low stiffness fluid at the normal fluid depth during (a,b) bubbling without valve oscillation and (c,d) bubbling with valve oscillations are shown in the same format as Figure 4. Red arrows indicate the pressure transient produced by bubble detachment from the nozzle, which is the most noticeable in PS1.

3.3. Deep Fluid Level

[23] In the low stiffness experiments performed at the normal fluid level, the temporary connectivity between the nozzle and the atmosphere via bubbles (Figure 7d) played an important role in energy transmission to the atmosphere. To investigate the effect of fluid depth, we doubled the depth of the low stiffness fluid. The primary effect of doubling the fluid depth is that bubbles detach from the conduit nozzle before reaching the fluid surface (Figure 10; Online Supplementary Video 4). Bubble detachment from the conduit nozzle produces a positive pressure pulse in the two conduit sensors, but the detachment is not transmitted into the atmosphere (Figure 10a). During both the bubbling regime and the bubbling plus valve oscillation regime, the deep fluid only permits the transmission of signals into the atmosphere through the oscillation of bubbles at the fluid surface. This prevents the momentary connection between the atmosphere and valve oscillation in the air conduit that was observed in the low stiffness, normal fluid depth experiments. The latency between bubble detachment and peak atmospheric pressure increases significantly with the onset of valve oscillation (Figures 10a and 10c). When the bubble reaches a critical volume, the drop in conduit pressure at the nozzle due to valve closure and the bubble buoyancy cause the bubble to pinch off the nozzle sooner than during constant conduit air pressure. As in the other experiments, bubbles bursting at the surface of the deeper fluid do not produce a significant pressure transient.

[24] The ΔT between subsequent valve oscillation pulses and the MaxXcorr between subsequent pairs of pressure pulses at PS1 were calculated and show that valve oscillation in the low stiffness, deeper fluid results in greater variability in timing and waveforms than in the same fluid at a shallower level (Figure 11). Whereas in the shallow fluid the timing between pulses and the similarity in the waveforms was only affected during bubble detaching (Figure 8), in the deeper fluid ΔT and MaxXcorr are constantly changing (Figure 11). Spectrograms of 10 s of data at MC1, PS1, and PS2 that span the bubbling and bubbling plus valve oscillation shown in Figure 10 are similar to those calculated for the low stiffness, shallow fluid (Figures 9 and 12). The vertical spectral stripes corresponding to bubble detachment in PS1 and PS2 and bubble oscillation at the fluid surface in MC1 are further apart and slightly more energetic due to the higher pressures associated with the deeper fluid. During

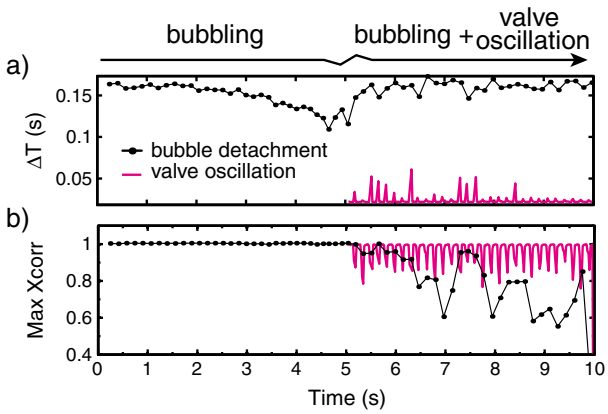

Figure 8. (a) Time interval (ΔT) and (b) maximum cross-correlation coefficient (MaxXcorr) between successive bubble detachments (black symbols) and valve oscillations recorded at PS1 during a10 s record spanning the activity shown in Figure 7. Time between bubble detachments drops over the first 5 s as air pressure is increased to initiate valve oscillation in Figure 8a, but the bubble waveforms remain very consistent in Figure 8b. The onset of valve oscillation increases ΔT between detachments in Figure 8a and the variability of the detachment waveforms in Figure 8b. Bubbles detaching from the nozzle cause an increase in the ΔT between oscillations in Figure 8a and a sharp drop in waveform similarity in Figure 8b.

valve oscillation, harmonic signals are present in the conduit pressure sensors, but the higher harmonics are distorted with broadband energy due to the irregularity of the pulse intervals (ΔT). Some faint energy below 200 Hz that corresponds to the energetic harmonics in PS1 is transmitted to the atmosphere despite no direct bubble connections from the conduit to the fluid surface (Figure 12a). We suspect that this energy was being transmitted directly though the fluid and coupling to the atmosphere at the fluid surface rather than being associated with the air bubbles.

4. Discussion

[25] Our experimental design allowed us to generate harmonic oscillations using a flow-driven valve, which has been invoked by several previous authors in models of volcanic HT generation [e.g., *Julian*, 1994; *Lees and Bolton*, 1998; *Lesage et al*., 2006; *Rust et al*., 2008]. Valve oscillation in the air conduit, which is analogous to SHT, is generated during all the experimental runs. However, the transmission of the harmonic oscillation into the atmosphere, analogous to SAHT, is only clearly observed when a connection is made between the air conduit and the atmosphere by means of an open channel or conduit in the viscoelastic fluid. The open conduit condition was only observed in experiments run with a high stiffness fluid. Some weak and unsteady HT was observed in the low fluid stiffness experiments when individual bubbles extended from the air conduit nozzle to the surface, but never sustained harmonics. While this simple experiment is not directly scalable to volcanic systems, the role of fluid stiffness and open channels in the viscoelastic fluid for controlling tremor transmission to the atmosphere can be related to active volcanoes and

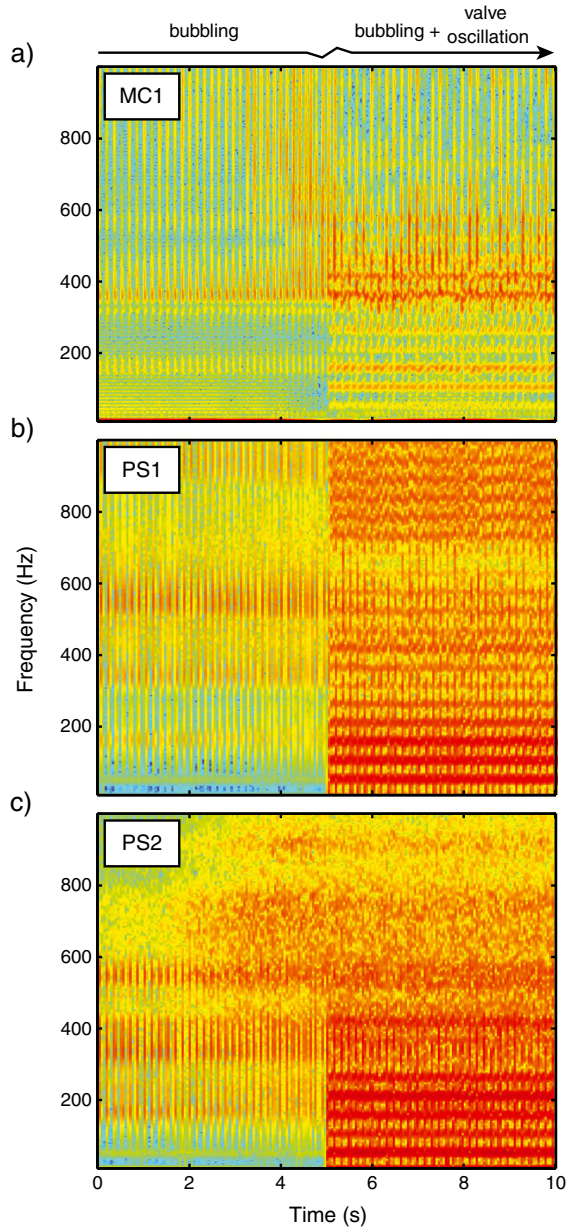

Figure 9. Spectrograms of bubbling and bubbling with valve oscillations in the low stiffness fluid at normal fluid depth for data recorded at (a) MC1, (b) PS1, and (c) PS2 during the same period shown in Figure 8. Bubbling alone produces broadband vertical stripes for each bubble detachment.

may help constrain under what conditions SHT – SAHT switching occurs.

[26] Persistent degassing plumes are a common feature at open vent volcanoes, even when magma is not being erupted. This is evidence that gas-rich magma in the conduit is capable of continuous degassing through pathways that may extend relatively deeply into the conduit [e.g., *Shinohara*, 2008]. In relatively low viscosity magmas, bubbles may rise more rapidly than the melt, coalesce, and eventually outgas at the surface via passive degassing, strombolian-style explosions or sustained lava fountains [*Jaupart and Vergniolle*, 1988; *Parfitt*, 2004]. In more viscous systems, gas bubbles and the melt are not expected

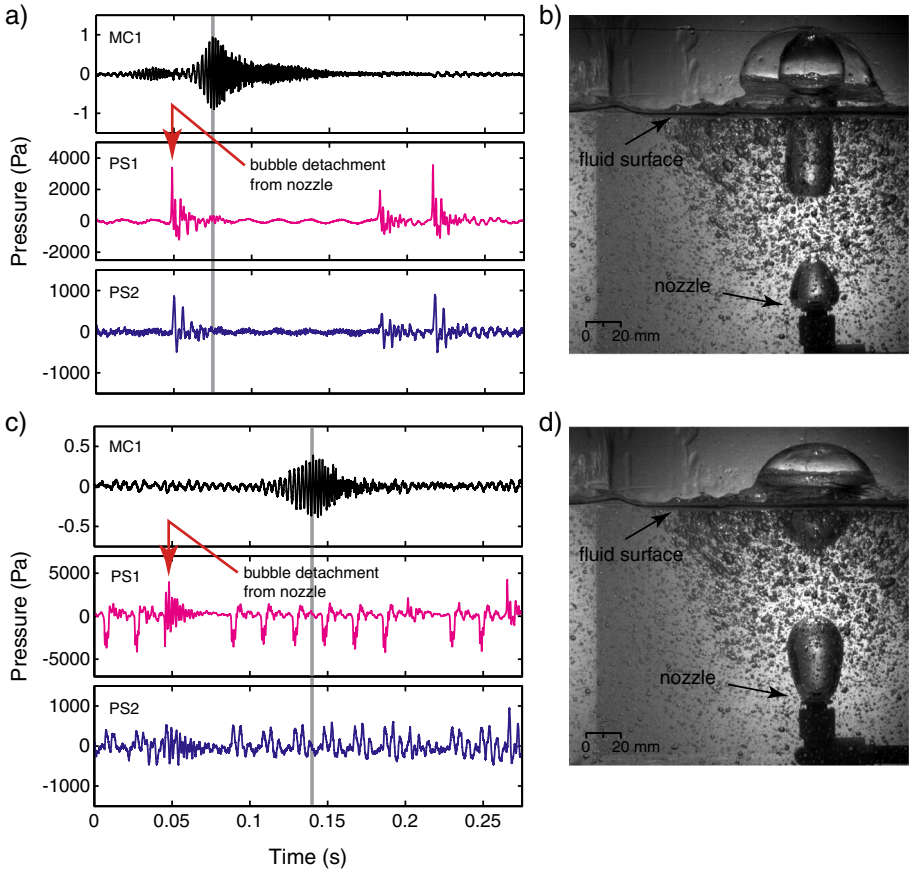

Figure 10. Waveforms and images of bubbling in the low stiffness fluid at the deep fluid depth during (a,b) bubbling without valve oscillation and (c,d) bubbling with valve oscillation are shown in the same format as Figures 4 and 7. The deeper fluid level results in bubbles detaching from the nozzle prior to reaching the surface both with and without valve oscillation. Bubbles rising to the surface and oscillating prior to bursting generate the pressure transients in MC1 both with and without valve oscillation in Figures 10a and 10c.

to move differentially so persistent degassing must be achieved through the permeability of the magma. Pervasive bubble networks and degassing channels formed by brittle failure along bubble channels have been observed or suggested to exist in the upper portions of magma columns based on field observations of dissected volcanic conduits [*Tuffen et al.*, 2003], numerical models [*Gonnermann and Manga*, 2003; *Melnik and Sparks*, 1999], laboratory experiments [*Okumura et al.*, 2008], and SO_2 measurements [*Edmonds et al.*, 2003]. HT has also been associated with observations of vigorous degassing through narrow cracks in dome carapaces at Galeras [*Cruz and Chouet*, 1997] and Santiaguito [*Johnson et al.*, 2009].

[27] Reports of SAHT are found at volcanoes with a wide range of magma viscosity, from basaltic andesite to dacite (e.g., Arenal [*Garcés et al.*, 1998; *Hagerty et al.*, 2000], Karymsky [*Johnson and Lees*, 2000; *Lees et al.*, 2004], Sangay [*Johnson and Lees*, 2000], and Santiaguito [*Johnson et al.*, 2009]). In contrast, lower viscosity basaltic volcanoes like Kilauea [*Fee and Garcés*, 2007; *Fee et al.*, 2010; *Garcés et al.*, 2003; *Matoza et al.*, 2010] and Villarrica [*Goto and Johnson*, 2011; *Ripepe et al.*, 2010] produce seismic and acoustic tremor that is monotonic or very weakly harmonic, lacking clear and abundant overtones. These observations, in conjunction with our experimental results, suggest that stable, open degassing pathways are unlikely to form in low viscosity magmas, and therefore SAHT is unlikely to be generated.

[28] The switching between SHT and SAHT is a more particular observation, which has only been previously observed in seismo-acoustic records from Reventador volcano, Ecuador [*Lees et al.*, 2008], Shinmoe-dake volcano, Japan [*Ichihara et al.*, 2012], and Arenal volcano, Costa Rica [*Hagerty et al.*, 2000], although never studied in detail. These volcanoes are all found in subduction-related arcs, produce intermediate-viscosity magmas, and have produced both effusive and explosive eruptive activity. The variability in eruption style at these volcanoes is likely associated with their ability to produce SHT – SAHT switching, but the underlying driver of switching has yet to be determined. In contrast, transitions back and forth between effusive and explosive behavior at volcanoes have been studied in more detail, and two general theories exists for what drives transitions, which may also provide insight into SHT – SAHT switching. The first is that relatively small variations in magma flux can affect a multitude of parameters in the conduit, which then act in concert to determine the eruptive style. These factors include: bubble size, growth and

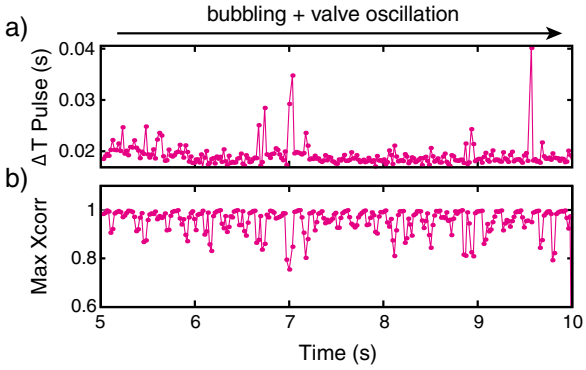

Figure 11. (a) Time interval (ΔT) and (b) maximum cross-correlation coefficient (MaxXcorr) between successive valve oscillations recorded at PS1 during a 5 s record spanning bubbling with valve oscillation shown in Figure 10c. The deeper fluid level resulted in more variable ΔT and MaxXcorr between valve oscillation signals than the same low stiffness fluid at the normal depth.

distribution, crystal content and nucleation rate and magma rheology [e.g., *Dingwell*, 1996; *Gonnermann and Manga*, 2007; *Melnik et al*., 2005; *Woods and Koyaguchi*, 1994]. The second is based on experiments performed by *Divoux et al*. [2009, 2011] in which they injected a Newtonian fluid into a non-Newtonian fluid to simulate gas in magma and observed intermittent switching between bubbling and an open conduit at a fixed fluid concentration and gas flux, which is attributed to the non-Newtonian properties of the fluid. They suggest that at some volcanoes, variations in eruptive style, particularly transitions between effusive and explosive behavior, may be controlled by the non-Newtonian nature of the magma rather than by changes in magma flux.

[29] In our experiment, the stiffness of the viscoelastic fluid was the dominant factor controlling whether open degassing channels were generated and remained open, which controlled whether SAHT was generated. Here we compare our experimental findings with an additional example of SHT – SAHT switching from Fuego volcano, Guatemala. Fuego erupts volatile-rich, intermediate viscosity basaltic andesite, often explosively [*Berlo et al*., 2012; *Lyons et al*., 2010; *Roggensack et al*., 1997]. We observed SHT during a period of strombolian activity in 2008 and SAHT during a period of weak vulcanian activity in 2009 (Figure 13). The seismo-acoustic record from 2008 shows more frequent, lower overpressure explosions than observed in 2009. A short active lava flow was also present in 2008, but there was no effusion in 2009. Gas emission data (SO_2) showed a slow, steady decrease prior to vulcanian-style explosions [*Nadeau et al*., 2011] concurrent with the onset of tilt as pressure accumulated prior to explosions [*Lyons and Waite*, 2011; *Lyons et al*., 2012]. These data are interpreted as more viscous magma in the uppermost portion of the conduit in 2009 than in 2008.

[30] We suggest that in 2009 a decreased magma supply rate led to a lower magma-static head and the development of a viscous plug at the top of the magma column, which developed the degassing pathways that allowed the generation of SAHT (Figure 13b). In contrast, a higher magma

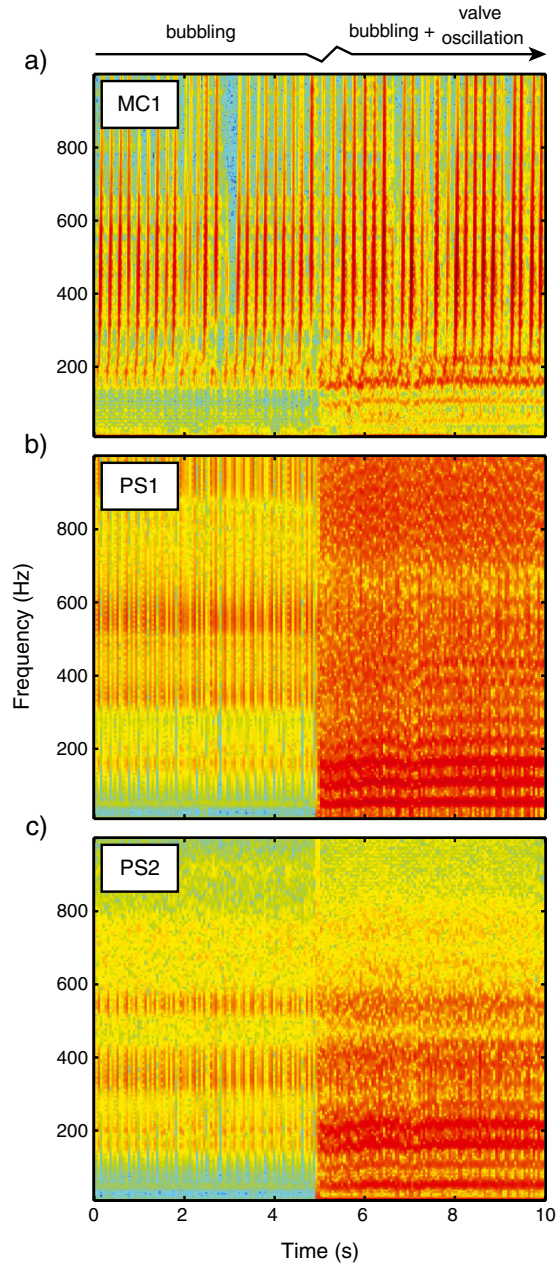

Figure 12. Spectrograms of bubbling and bubbling with valve oscillation in the low stiffness fluid at normal fluid depth for data recorded at (a) MC1, (b) PS1, and (c) PS2 starting 5 s before the period in Figure 11. Bubbling alone produces broadband vertical stripes for each bubble detachment in PS1 and PS2 and bubble oscillations at the fluid surface in MC1.

supply rate in 2008 resulted in strombolian explosions and effusion and prevented an increase in viscosity and stable degassing pathways, only generating SHT (Figure 13a). However, both our experimental results and our observations at Fuego are limited. Future work on samples collected during both SHT and SAHT is needed to determine if the effective viscosity is significantly different, or if some other factor is dominant. In a companion study, results suggest that similar shallow conduit dynamics may also be responsible for SHT – SAHT switching observed at Shinmoe-dake

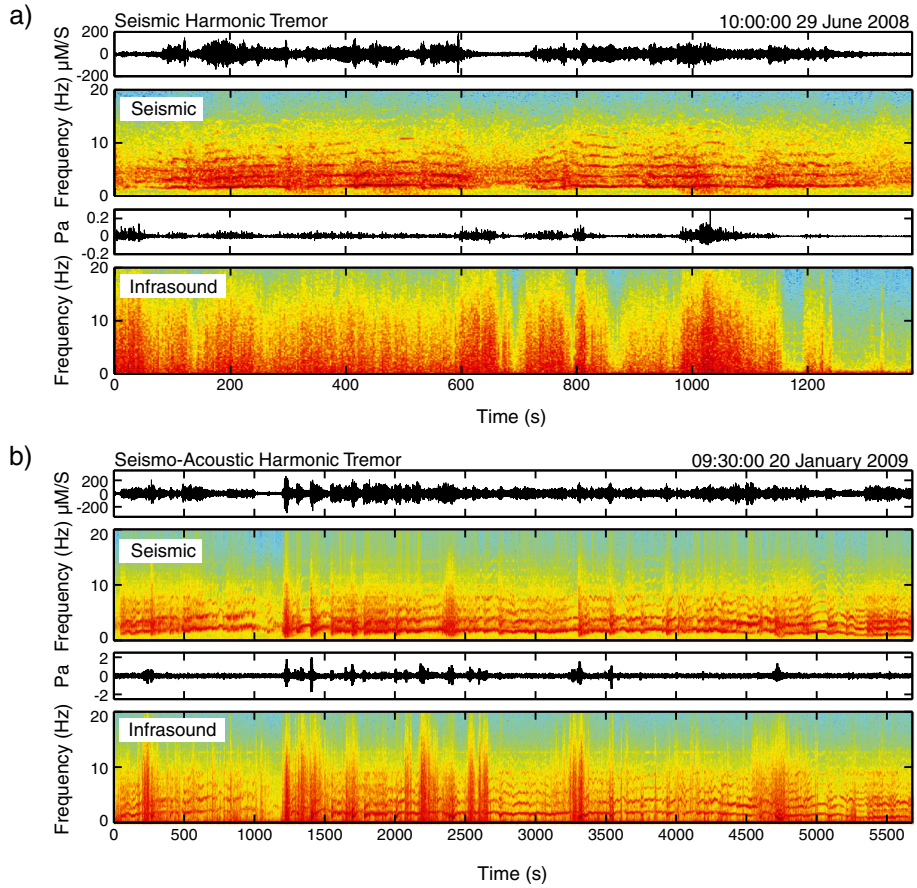

Figure 13. Waveforms and spectrograms of seismic and infrasound data recorded 750 m from the summit vent at Fuego volcano in (a) 2008 when seismic harmonic tremor dominated and (b) in 2009 when seismo-acoustic harmonic tremor dominated. The change in the harmonic tremor records was accompanied by a clear shift in eruptive behavior from frequent strombolian explosions and active lava effusion in 2008 to more vulcanian activity in 2009 with fewer but stronger explosions and no effusion.

volcano [*Ichihara et al.*, Switching from SHT to SAHT at a transition of eruptive activity, *submitted to Earth, Planets and Space*, 2012]. However, observations of switching at other volcanoes and continued experimental advances are needed to more fully understand SHT – SAHT switching.

5. Conclusions

[31] We present results from a series of laboratory experiments designed to simulate the previously unexplained switching between SHT and seismic and infrasonic HT, which has been observed at Fuego, Shinmoe-dake, Arenal and Reventador volcanoes. The experimental design was inspired by theoretical models for flow-driven HT in volcanoes and previous laboratory experiments. The harmonic signal was generated by the flow of compressed air through a valve, which was located below a tank of viscoelastic fluid. Pressure fluctuations generated by the flow of air through the valve system were recorded on pressure sensors isolated from the atmosphere, while energy transmitted through the fluid and into the atmosphere were recorded on microphones. Valve oscillation, analogous to SHT, was produced in all the experimental runs, but clear harmonic oscillation and the efficient transmission of the oscillation signal into the atmosphere was only observed when stable, open channels were generated in an adequately high stiffness fluid. Experiments run with lower viscosity fluid were dominated by bubbling and never produced stable harmonics in the atmosphere.

[32] These results are compared with two seismo-acoustic records at Fuego volcano, which showed a striking change in eruptive behavior from effusion and strombolian explosions in 2008 to vulcanian explosions without effusion in 2009. Previous studies of the 2009 activity cite shallow changes in rheology driven by degassing crystallization and volatile loss to explain the eruptive behavior. Based on the eruption observations and experimental results, we surmise that a subtle change in magma supply rate drove the change from strombolian to vulcanian activity. This change is recorded in the seismo-acoustic data as a switch from predominately SHT to SAHT as the effective viscosity increased and stable degassing pathways formed in the top of the magma column. Similar observations at Shinmoe-dake suggest that SHT – SAHT switching may be common at intermediate viscosity volcanoes and may be indicative of changes in shallow conduit dynamics. Laboratory experiments capable of reproducing geophysical signals that are difficult or impossible to directly observe in nature provide a powerful tool for visualizing and elucidating conduit and eruption dynamics.

[33] **Acknowledgments.** The authors would like to thank the National Science Foundation Office of International Science and Engineering East Asia and Pacific Summer Institutes Program and the Japan Society for the Promotion of Science for supporting the experimental work and travel expenses. Thanks to Minoru Takeo for support of JJL's field and laboratory work while in Japan, as well as discussions that improved the manuscript. We gratefully acknowledge field support at Fuego volcano from Edgar Barrios, Kyle Brill, Chris Brown, Amilcar Calderas, Gustavo Chigna, Mari Dalton, Jemile Erdem, Tricia Nadeau, Josh Richardson, Jesse Silverman, and INSIVUMEH. Thanks to Greg Waite for stimulating discussions about Fuego's tremor. Thoughtful reviews by the Associate Editor Micol Todesco and two anonymous reviewers helped to significantly improve the paper.

References

Benoit, J. P., and S. R. McNutt (1997), New constraints on source processes of volcanic tremor at Arenal Volcano, Costa Rica, using broadband seismic data, *Geophys. Res. Lett.*, *24*(4), 449–452.

Berlo, K., J. Stix, K. Roggensack, and B. Ghaleb (2012), A tale of two magmas, Fuego, Guatemala, *Bull. Volcanol.*, *74*(2), 377–390, doi:10.1007/s00445-011-0530-8.

Chouet, B. (1988), Resonance of a fluid-driven crack: Radiation properties and implications for the source of long-period events and harmonic tremor, *J. Geophys. Res.*, *93*(B5), 4347–4400.

Cruz, F. G., and B. A. Chouet (1997), Long-period events, the most characteristic seismicity accompanying the emplacement and extrusion of a lava dome in Galeras Volcano, Colombia, in 1991, *J. Volcanol. Geotherm. Res.*, *77*(1-4), 121–158, doi:10.1016/s0377-0273(96)00091-1.

Dingwell, D. B. (1996), Volcanic dilemma: Flow or blow?, *Science*, *v273*(n5278), p1054(1052).

Divoux, T., E. Bertin, V. Vidal, and J.-C. Géminard (2009), Intermittent outgassing through a non-Newtonian fluid, *Phys. Rev. E*, *79*(5), 056204, doi:10.1103/PhysRevE.79.056204.

Divoux, T., V. Vidal, M. Ripepe, and J.-C. Géminard (2011), Influence of non-Newtonian rheology on magma degassing, *Geophys. Res. Lett.*, *38*(12), L12301, doi:10.1029/2011gl047789.

Edmonds, M., C. Oppenheimer, D. M. Pyle, R. A. Herd, and G. Thompson (2003), SO_2 emissions from Soufrière Hills Volcano and their relationship to conduit permeability, hydrothermal interaction and degassing regime, *J. Volcanol. Geotherm. Res.*, *124*(1–2), 23–43, doi:10.1016/s0377-0273(03)00041-6.

Fee, D., and M. Garcés (2007), Infrasonic tremor in the diffraction zone, *Geophys. Res. Lett.*, *34*(16), L16826, doi:10.1029/2007gl030616.

Fee, D., M. Garcés, M. Patrick, B. Chouet, P. Dawson, and D. Swanson (2010), Infrasonic harmonic tremor and degassing bursts from Halema'uma'u Crater, Kilauea Volcano, Hawaii, *J. Geophys. Res.*, *115*(B11), B11316, doi:10.1029/2010jb007642.

Fehler, M. (1983), Observations of volcanic tremor at Mount St. Helens Volcano, *J. Geophys. Res.*, *88*(B4), 3476–3484, doi:10.1029/JB088iB04p03476.

Fletcher, N., and T. D. Rossing (1998), The Physics of Musical Instruments, Springer-Verlag, New York.

Fletcher, N. H. (1993), Autonomous vibration of simple pressure-controlled valves in gas flows, *J. Acoust. Soc. Am.*, *93*(4), 2172–2180.

Garcés, M., A. Harris, C. Hetzer, J. Johnson, S. Rowland, E. Marchetti, and P. Okubo (2003), Infrasonic tremor observed at Kilauea Volcano, Hawai'i, *Geophys. Res. Lett.*, *30*(20), doi:10.1029/2003GL018038.

Garcés, M. A., M. T. Hagerty, and S. Y. Schwartz (1998), Magma acoustics and time-varying melt properties at Arenal Volcano, Costa Rica, *Geophys. Res. Lett.*, *25*(13), 2293–2296, doi:10.1029/98gl01511.

Gonnermann, H. M., and M. Manga (2003), Explosive volcanism may not be an inevitable consequence of magma fragmentation, *Nature*, *426*(6965), 432–435, doi:10.1038/nature02138.

Gonnermann, H. M., and M. Manga (2007), The fluid mechanics inside a volcano, *Annu. Rev. Fluid Mech.*, *39*(1), 321–356, doi:10.1146/annurev.fluid.39.050905.110207.

Gordeev, E. (1993), Modeling of volcanic tremor as explosive point sources in a single-layered, elastic half-space, *J. Geophys. Res.*, *98*, doi:10.1029/93jb00348.

Goto, A., and J. B. Johnson (2011), Monotonic infrasound and helmholtz resonance at Volcan Villarrica (Chile), *Geophys. Res. Lett.*, *38*(6), L06301, doi:10.1029/2011gl046858.

Hagerty, M. T., S. Y. Schwartz, M. A. Garcés, and M. Protti (2000), Analysis of seismic and acoustic observations at Arenal Volcano, Costa Rica, 1995–1997, *J. Volcanol. Geotherm. Res.*, *101*(1-2), 27–65.

Ichihara, M., J. Lyons, J. Oikawa, and M. Takeo (2012), Acoustic waves in the atmosphere and ground generated by volcanic activity, paper presented at The 19th International Symposium on Nonlinear Acoustics, Tokyo, Japan.

Jaupart, C., and S. Vergniolle (1988), Laboratory models of Hawaiian and Strombolian eruptions, *Nature*, *331*(6151), 58–60.

Johnson, J. B., and J. M. Lees (2000), Plugs and chugs—Seismic and acoustic observations of degassing explosions at Karymsky, Russia and Sangay, Ecuador, *J. Volcanol. Geotherm. Res.*, *101*(1–2), 67–82, doi:10.1016/s0377-0273(00)00164-5.

Johnson, J. B., R. Sanderson, J. Lyons, R. Escobar-Wolf, G. Waite, and J. M. Lees (2009), Dissection of a composite volcanic earthquake at Santiaguito, Guatemala, *Geophys. Res. Lett.*, *36*, doi:10.1029/2009gl039370.

Julian, B. R. (1994), Volcanic tremor: Nonlinear excitation by fluid flow, *J. Geophys. Res.*, *99*(B6), 11,859–811,878, doi:10.1029/93JB03129.

Lees, J. M., and E. W. Bolton (1998), Pressure cookers as volcano analogues, in EOS, Trans. Am. Geophys. Un., edited, p. 620, American Geophysical Union, San Francisco, Calif.

Lees, J. M., E. I. Gordeev, and M. Ripepe (2004), Explosions and periodic tremor at Karymsky Volcano, Kamchatka, Russia, *Geophys. J. Int.*, *158*(3), 1151–1167, doi:10.1111/j.1365-246X.2004.02239.x.

Lees, J. M., J. B. Johnson, M. Ruiz, L. Troncoso, and M. Welsh (2008), Reventador Volcano 2005: Eruptive activity inferred from seismo-acoustic observation, *J. Volcanol. Geotherm. Res.*, *176*(1), 179–190, doi:10.1016/j.jvolgeores.2007.10.006.

Lesage, P., M. M. Mora, G. E. Alvarado, J. Pacheco, and J.-P. Métaxian (2006), Complex behavior and source model of the tremor at Arenal Volcano, Costa Rica, *J. Volcanol. Geotherm. Res.*, *157*, 49–59, doi:10.1016/j.jvolgeores.2006.03.047.

Lyons, J., G. Waite, W. Rose, and G. Chigna (2010), Patterns in open vent, Strombolian behavior at Fuego Volcano, Guatemala, 2005–2007, *Bull. Volcanol.*, *72*(1), 1–15, doi:10.1007/s00445-009-0305-7.

Lyons, J. J., and G. P. Waite (2011), Dynamics of explosive volcanism at Fuego Volcano imaged with very long period seismicity, *J. Geophys. Res.*, *116*(B9), B09303, doi:10.1029/2011jb008521.

Lyons, J. J., G. P. Waite, M. Ichihara, and J. M. Lees (2012), Tilt prior to explosions and the effect of topography on ultra-long-period seismic records at Fuego Volcano, Guatemala, *Geophys. Res. Lett.*, *39*(8), L08305, doi:10.1029/2012gl051184.

Matoza, R. S., D. Fee, and M. A. Garcés (2010), Infrasonic tremor wavefield of the Pu`U `Ō`Ō; Crater complex and lava tube system, Hawaii, in April 2007, *J. Geophys. Res.*, *115*(B12), B12312, doi:10.1029/2009jb007192.

McNutt, S. R. (1994), Volcanic tremor from around the World: 1992 update, *Acta Vulcanol*, *5*, 197–200.

Melnik, O., and R. S. J. Sparks (1999), Nonlinear dynamics of lava dome extrusion, *Nature*, *402*(6757), 37–41, doi:10.1038/46950.

Melnik, O., A. A. Barmin, and R. S. J. Sparks (2005), Dynamics of magma flow inside volcanic conduits with bubble overpressure buildup and gas loss through permeable magma, *J. Volcanol. Geotherm. Res.*, *143*, 53–68, doi:10.1016/j.jvolgeores.2004.09.010.

Mori, J., H. Patia, C. McKee, I. Itikarai, P. Lowenstein, P. De Saint Ours, and B. Talai (1989), Seismicity associated with eruptive activity at Langila Volcano, Papua New Guinea, *J. Volcanol. Geotherm. Res.*, *38*(3-4), 243–255.

Nadeau, P. A., J. L. Palma, and G. P. Waite (2011), Linking volcanic tremor, degassing, and eruption dynamics via So2 imaging, *Geophys. Res. Lett.*, *38*(1), L01304, doi:10.1029/2010gl045820.

Okumura, S., M. Nakamura, A. Tsuchiyama, T. Nakano, and K. Uesugi (2008), Evolution of bubble microstructure in sheared rhyolite: Formation of a channel-like bubble network, *J. Geophys. Res.*, *113*(B7), B07208, doi:10.1029/2007jb005362.

Parfitt, E. A. (2004), A discussion of the mechanisms of explosive basaltic eruptions, *J. Volcanol. Geotherm. Res.*, *134*(1-2), 77–107, doi:10.1016/j.jvolgeores.2004.01.002.

Ripepe, M., E. Marchetti, C. Bonadonna, A. J. L. Harris, L. Pioli, and G. Ulivieri (2010), Monochromatic infrasonic tremor driven by persistent degassing and convection at Villarrica Volcano, Chile, *Geophys. Res. Lett.*, *37*(15), L15303, doi:10.1029/2010gl043516.

Roggensack, K., R. L. Hervig, S. B. McKnight, and S. N. Williams (1997), Explosive basaltic volcanism from Cerro Negro Volcano: Influence of volatiles on eruptive style, *Science 277*, 1639–1642.

Rust, A. C., N. J. Balmforth, and S. Mandre (2008), The feasibility of generating low-frequency volcano seismicity by flow through a deformable channel, *Geol. Soc., London, Spec. Publ.*, *307*(1), 45–56, doi:10.1144/sp307.4.

Sakai, T., H. Yamasato, and K. Uhira (1996), Infrasound accompanying C-type tremor at Sakurajima Volcano (in Japanese), *Bull. Volcanol. Soc. Jpn.*, *41*, 181–185.

Schlindwein, V., J. Wassermann, and F. Scherbaum (1995), Spectral analysis of harmonic tremor signals at Mt. Semeru Volcano, Indonesia, *Geophys. Res. Lett.*, *22*(13), 1685–1688.

Shinohara, H. (2008), Excess degassing from volcanoes and its role on eruptive and intrusive activity, *Rev. Geophys.*, *46*, doi:10.1029/2007rg000244.

Tuffen, H., D. B. Dingwell, and H. Pinkerton (2003), Repeated fracture and healing of silicic magma generate flow banding and earthquakes?, *Geology*, *31*(12), 1089–1092, doi:10.1130/g19777.1.

Vidal, V., M. Ichihara, M. Ripepe, and K. Kurita (2009), Acoustic waveform of continuous bubbling in a non-Newtonian fluid, *Phys. Rev. E*, *80*(6), 066314.

Woods, A. W., and T. Koyaguchi (1994), Transitions between explosive and effusive eruptions of silicic magmas, *Lett. Nat.*, *370*, 641–644.

Yokoo, A., T. Tameguri, M. Iguchi, and K. Ishihara (2008), Sequence and characteristics of the 2007 eruption at Showa Crater of Sakurajima Volcano (in Japanese with English abstract), *Ann. Disas. Prev. Res. Inst., Kyoto Univ.*, *51B*, 267–273.